Optical Solitons in Topological SSH Waveguides

Ju Won Choi[1], Byoung-Uk Sohn[1], Hongwei Gao[1], George F. R. Chen[1], Jia Sheng Goh[2], Doris K. T. Ng[2], and Dawn T. H. Tan[1,*]

[1]*Photonics Devices and System Group, Singapore University of Technology and Design, 8 Somapah Rd, Singapore 487372, Singapore*
[2]*Institute of Microelectronics, Agency for Science Technology and Research (A*STAR), 2 Fusionopolis Way, #08-02, Innovis Tower, Singapore 138634, Singapore*
dawn_tan@sutd.edu.sg

Abstract: We demonstrate optical temporal solitons using topological Su-Schrieffer-Heeger waveguides implemented on ultra-silicon-rich nitride with high Kerr nonlinearity and negligible nonlinear loss at a wavelength of 1550nm, achieving 2x temporal compression of 0.97ps pulses.

1. Introduction

Topological solitons, first observed in the Su-Schrieffer-Heeger (SSH) system, represented a major advance in condensed matter physics, comparable to the discovery of anomalous Hall conductance in periodic systems [1]. Topological waveguides in photonics exploit zero modes formed at interfaces between different topological domains in dimerized lattices. The 1D SSH model features two sites per unit cell, with topology determined by the relative strength of intracell (v) and intercell (w) coupling. The interface between regions of differing topological properties creates a domain wall, generating a topological mode whose peak aligns with the boundary [2].

Ultra-silicon-rich nitride (USRN), a CMOS-compatible platform with high Kerr nonlinearity (n_2 = 2.8x10^{-13} cm^2/W) and negligible nonlinear loss near 1550 nm [3,4], has enabled various soliton phenomena. Recently, we demonstrated efficient optical parametric amplification using strong light confinement in a USRN topological waveguide based on the SSH model with a domain wall [2], revealing that the Kerr effect could induce topological mode delocalization.

In this work, we investigate optical temporal solitons in USRN topological waveguides, focusing on the boundary waveguide where light confinement is strongest. We demonstrate 2x temporal compression at an input peak power of 45.3W. The boundary waveguide exhibits output power saturation for input pulses of < 1ps, consistent with previous findings. To explain the temporal soliton behaviour, we employed nonlinear Schrödinger equation simulations, incorporating a reduced power factor in a single waveguide, yielding theoretical compression factors that agree well with experimental results [5].

2. Results and discussion

We designed a USRN-based topological photonic waveguide based on the SSH model with a domain wall as shown in Fig. 1 (a). The device comprises 199 waveguides, providing an adequate transverse dimension to ensure for the localized boundary mode that spans 9 waveguides. Each waveguide has a width and height of 600nm and 340nm respectively, with G_w = 0.15µm and G_v = 0.25µm, optimized for strong localization with a coupling ratio v/w = 0.17 [2].

Optical pulses of 0.93 ps were employed to investigate the temporal soliton, allowing power-based control of the topological mode. The device's output average power is measured relative to the input coupled average power as shown in Fig. 1(b). Due to the SSH structure's constant propagation loss throughout the transmission, the reduced power factor ($\eta(P_{in})$) shows a decrease with increasing input power as illustrated in Fig. 1(c). The measured output power agrees well with theoretical predictions (blue line in Fig.1(b)), showing the power-dependent nature of η.

To analyze optical pulse propagation in SSH-distributed spatial coupled waveguides, we employ the nonlinear Schrödinger equation (NLSE) in a single waveguide for numerical analysis. When light enters through the central waveguide, it can excite both the dominant topological boundary mode and bulk modes, with the nonlinear Kerr effect modifying the topological boundary mode by increasing the localized effective index, leading to a reduction in its amplitude at the boundary waveguide. In our NLSE simulations, we apply the modified input peak power term to $P_{in}*\eta(P_{in})$ based on Fig. 1(c) to study temporal pulse propagation at the boundary waveguide.

Figure 2(a) displays experimental output temporal traces obtained by applying a deconvolution factor of 1.54 (for $sech^2$ pulse) to autocorrelation traces. While exact comparisons between experimental and theoretical temporal

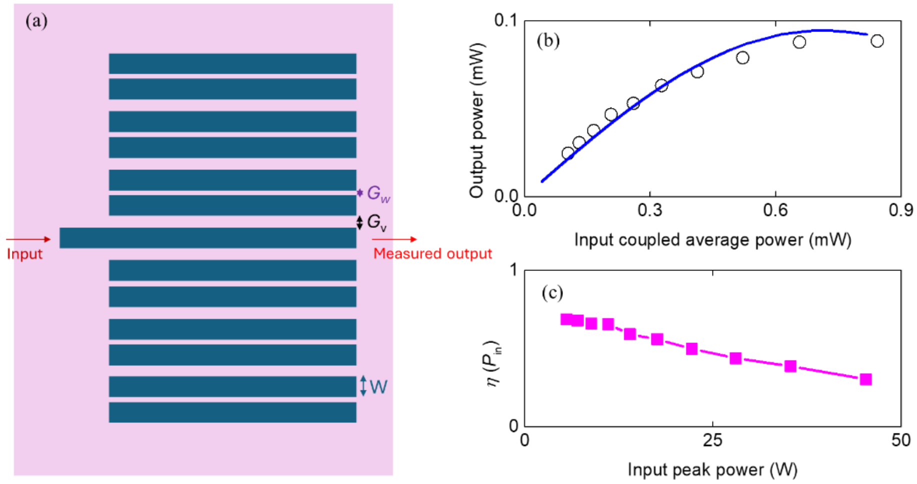

Fig. 1. (a) Schematic representation of the topological waveguide with a domain wall (where light enters and exits through the central (boundary) waveguide). (b) Experimental output power as a function of input coupled average power (empty circle), with theoretical calculations based on the NLSE shown in blue line. (c) Reduced power factor (η) as a function of input coupled peak power.

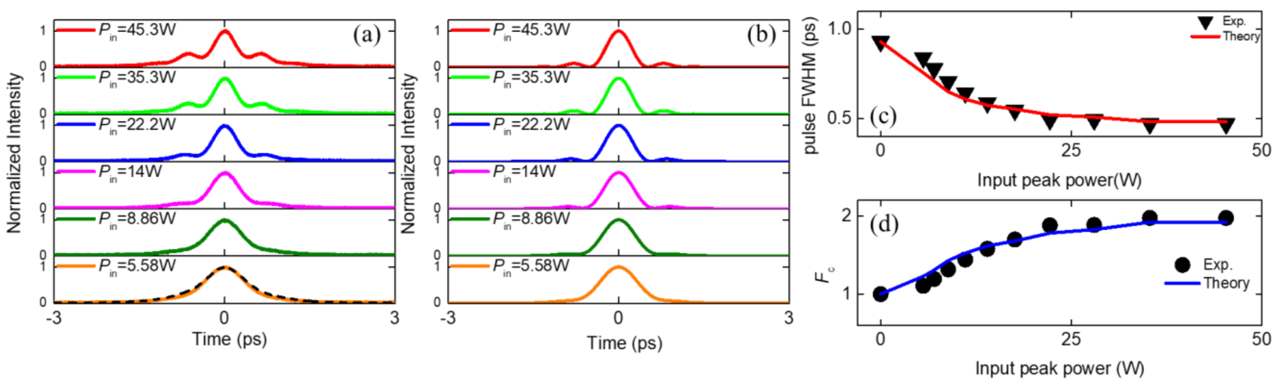

Fig. 2. (a) Experimental and (b) theoretical output temporal traces are shown as a function of input peak power. The experimental traces are derived by applying deconvolution factors to autocorrelation traces to enable pulse width comparison between theory and experiment. Input pulse is shown as a black dashed line in Fig. 2(a). (c) Comparison of experimental pulse FWHM (black triangles) with theoretical predictions (red line) as a function of input peak powers (d) The compression factor (F_c) that is experimentally measured (black circles) and the corresponding theoretical predictions (blue line) as input peak power varies.

traces aren't possible, we can compare their pulse widths. Figure 2(b) shows the theoretical temporal traces derived from the NLSE. Based on Fig. 2 (a) and (b), theoretical and experimental pulse full width half maximum (FWHM) are compared as shown in Fig. 2(c). The theoretical and experimental pulse widths agree well with each other. For an input peak power of 45.3 W, a minimum pulse width of 0.47 ps is achieved, representing a compression factor of 1.98, as demonstrated in Fig. 2(d). This agreement confirms that NLSE incorporating the reduced power factor can explain well the temporal soliton behavior in an SSH boundary waveguide.

Acknowledgments: Funding from the National Research Foundation Investigatorship (NRF-NRFI08-2022-0003), Agency for Science, Technology and Research under grant no. M23M5a0069 for device fabrication, characterization, Ministry of Education ACRF Tier 2 Grant (T2EP50121-0019) and the Quantum Engineering Programme 2.0 grant (NRF2022-QEP2-01-P08) is gratefully acknowledged.

3. References

[1] W. P. Su, J. Schrieffer, and A. J. Heeger, Phys. Rev. Lett. **42**, 1698-1701 (1979).
[2] B.-U. Sohn, et al., Nat. Commun. 13, 7218 (2022).
[3] T. Wang, et al., Laser Photonics Rev. **9**, 498–506 (2015).
[4] B.-U. Sohn, et al., Sci. Rep. **9**, 1–7 (2019).
[5] J. W. Choi, et al., Sci. Rep. **14,** 28074 (2024).